EXPERIMENTAL VALIDATION OF EQUIVALENT CIRCUIT MODELLING OF THE PIEZO-STRIPE HARVESTER ATTACHED TO THE SFSF RECTANGULAR PLATE

Andrzej KOSZEWNIK*

*Faculty of Mechanical Engineering, Department of Robotics Systems and Mechatronics, Wiejska 45C, 15-351 Białystok, Poland

a.koszewnik@pb.edu.pl

received 23 September 2019, revised 1 March 2020, accepted 4 March 2020

Abstract: Plate-like structures with attached piezo-patch elements are widely used in marine, aerospace and civil infrastructure applications to power small devices with low power demand or used for monitoring of vibration structures. In order to assess the feasibility of an energy harvesting system to generate power output from a harvester, an accurate electromechanical model of the piezo-patch harvester attached to a 2D structure in modal coordinates is required. Taking into account this fact, this study is focused on the analysis of the piezo-harvester orientations on the SFSF (Simply Supported-Free-Simply Supported-Free) plate undergoing forced dynamic excitation. The results obtained from the numerical analysis of a smart structure led to determining quasi-optimal piezo-harvester location on the structure, and next, to determining a multi-mode representation of the equivalent circuit model. The experimental set-up carried out on the lab stand properly verified the parameters of the ECM model. Finally, the proposed approach can be used for the structural health monitoring of vibration of some 2D mechanical structures like the front wall of a dishwasher.

Keywords: Aluminium plate, piezo-harvester, energy harvesting system, modal analysis, Equivalent Circuit Model (ECM)

1. INTRODUCTION

The number of applications of self-powered wireless sensors and health monitoring systems has been growing increasingly because the external power requirement has reduced to the micro-watt range in the past two decades (Koszewnik, 2019; Hu and Zhang, 2011). As a result, vibration-based energy harvesting systems have become a promising approach to provide constant power supply of low power electronics (Roundy et al., 2003). Taking into account the scope of some references, it is well known that this effect can be achieved by using different types of transduction mechanisms like electromagnetic (Naifar et al., 205; A,nrożiewicz et al., 2020), electrostatic (Chiu and Tseng, 2008; Lee et al., 2009), magnetostrictive (Wang and Yuan, 2008) and piezoelectric (Okosun et al., 2019; Koszewnik and Wernio, 2016). However, only piezoelectric energy harvesting transducers have drawn more attention due to the ease of their fabrication and the possibility to be applied in microsystems and macroscale devices (Cook-Chennault et al., 2007).

Generally, the piezoelectric energy harvesting systems are strongly focused on analysing 1D structures with piezo-ceramic layers, due to the fact that they are easy to model and implement (Borowiec, 2015). For this reason, analytical and numerical models of cantilever beams with a perfectly bonded piezo-harvester have been extensively developed by several research groups. For instance, analytical distributed–parameter modelling of beams for chaotic vibration with experimental set-up were presented in reference (Litak et al., 2009), while modelling of a self-resonating energy harvester system of cantilever beams with identification and experimental investigations in Aboulfotoh et al. (2017). In other practical implementations, the EH system is used to monitor water pipes as a novel technology for leak detection (Okosun et al., 2019).

As compared to the number of studies dealing with piezoelectric harvester beams, research on 2D structures with an attached piezoceramic patch harvester is very limited (Gosiewski, 2008). For instance, Marqui presented an electromechanical finite element model for a PEH embedded in a cantilever plate, and later on extended this model with airflow excitation problems by electroelastic coupling for energy harvesting from aeroelastic flutter (De Marqui, 2011). We have found a similar application in the paper published by Anton, who was the first to design and investigate novel piezoelectric devices installed on UAV platforms. For instance, the author in reference (Anton Nove, 2019) showed a piezoelectric patch with a thin-film battery as a multifunctional self-charging device for scavenging energy. Later, the same author presented a hybrid device, containing piezo-electric stripes, macro-fibre and piezo-fibre composites, that allows harvesting energy from wing vibrations (Anton, 2011).

The results obtained in these investigations led to further development of this research area and their applications for civil structures. For instance, Harne modelled electroelastic dynamics of a vibrating panel with a corrugated piezoelectric spring and then analysed this corrugated harvester device by attaching it to a panel of public bus (Hantre, 2012, 2013). In other papers, authors used vibration energy harvesting devices for monitoring a full-scale bridge as a 2D structure undergoing forced dynamic vibrations generated by vehicle or passenger trains going over them (Cahill et al., 2014,2018). An additional advantage of this is the fact that the harvested energy can be used to sufficiently power other small devices with low power demand.

The results obtained from the above papers and monitoring of civil infrastructure (bridge) by using longitudinally located piezo

DOI 10.2478/ama-2020-0002

harvesters gave motivation to analyse the harvester locations and orientations on the structure and assess the energy harvesting system effectiveness. In order to do this, firstly, the mechanical strains of the structure considered in this paper were analysed for two perpendicular directions. This allowed to indicate the best piezo-harvester locations and orientations on the structure and determine the electromechanical model of the whole structure. Additionally, the experimental test carried out on the lab stand allowed to verify the numerical results and showed that this approach can be used to assess voltage generating by the piezo-harvester. As a result, the proposed approach enables exploiting the harvesting capabilities of the piezoelectric patch-based harvester attached to a thin rectangular plate with any linear and nonlinear electrical components. Moreover, multi-vibration mode equivalent circuit model of the PZT patch-based harvesters, determined in this way, also allow to simplify the optimization process of these systems in order to maximize the power output. As a result, the proposed approach filled the gap in modelling EH systems for 2D structures, and it enables designing structural health monitoring systems of some structures, like dishwashers.

2. ANALYTICAL DISTRIBUTED PARAMETER MODEL OF SFSF PLATE WITH HARVESTER

The analytical distributed-parameter model of the SFSF plate with a perfectly bonded piezo patch harvester is presented in this Section. For this purpose, all parameters of the whole smart structure are firstly collected in Tab. 1, and then, the model of this structure based on the parameters and by using the Kirchhoff's plate theory is determined.

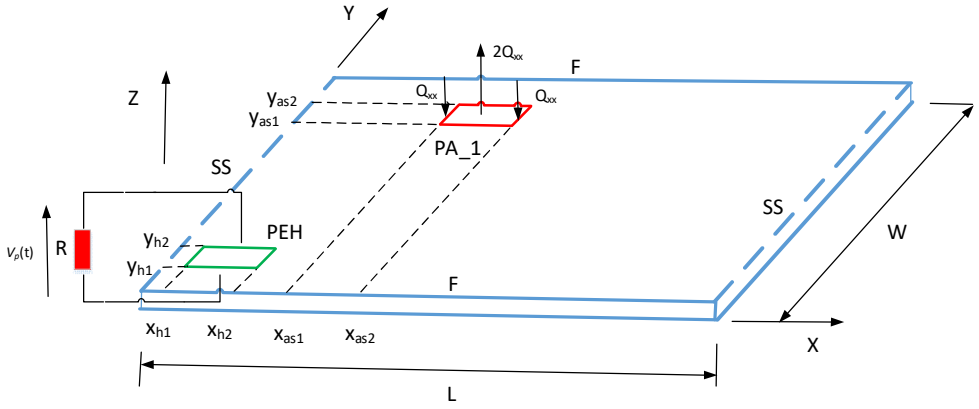

Fig. 1. The host plate with piezo-patches working as a harvester (PEH) and actuator – PA_1

Tab. 1. Parameters of the host structure and piezo-stripes (Koszewnik, 2016)

Parameter	Plate		Piezo-element	Actuator QP20N	Harvester V21BL
Length [m]	L	0.4	l_p / l_{peh}	0.05	0.048
Width [m]	W	0.2	w_p / w_{peh}	0.025	0.0125
Thickness [m]	h_{plate}	0.0002	h_a / h_{peh}	0.000782	0.000787
Young module [GPa]	E_b	70	E_p	0.18	0.18
Density [kg/m^3]	ρ_{plate}	2720	ρ_p	7200	7200
strain constant of piezo [pm/V]	-	-	d_{33}	-125	-
piezoelectric stress/charge constant [pC/m^2]	-	-	e_{31}	-	-6.5

As it can be seen in Fig. 1, the plate is excited to vibrations by the piezo actuator covering the surface of the plate at corners (xas1,yas1) and (xas2,yas2). As a result, the whole plate is excited to vibration by the bending moment Mx(x,y) at the position of the actuator. The piezo-harvester (PEH) with the length of (l_{peh}), the width of (w_{peh}) and the thickness of (h_{peh}), was additionally integrated with the structure at the positions (xh1,yh1) and (xh2, yh2) in order to measure voltage from the vibrations. As a result, by assuming an external electrical load (a resistive load R), and the piezo-stripe element coupling with the host structure only electromechanically, the transverse vibration of the smart plate can be expressed in the following form (De Marqui, 2011):

$$D\left(\frac{\partial^4 w(x,y,t)}{\partial x^4}+2\frac{\partial^4 w(x,y,t)}{\partial x^2 y^2}+\frac{\partial^4 w(x,y,t)}{\partial x^4}\right)+c\frac{\partial w(x,y,t)}{\partial t}+\rho_{peh}h_{peh}\frac{\partial^2 w(x,y,t)}{\partial t^2}$$

$$-\Gamma V_p(t)\left\{\begin{bmatrix}\frac{d\delta(x-x_{h1})}{dx}-\frac{d\delta(x-x_{h2})}{dx}\end{bmatrix}\times[H(y-y_{h1})-H(y-y_{h2})]+\right.\\ \left.\begin{bmatrix}\frac{d\delta(y-y_{h1})}{dy}-\frac{d\delta(y-y_{h2})}{dy}\end{bmatrix}\times[H(x-x_{h1})-H(x-x_{h2})]\right\}=\left[\frac{\partial^2 M_x(x,y)}{\partial x^2}\right] \quad (1)$$

where h_{peh} denotes the thickness of the harvester, ρ_{peh} – the density of the harvester, D – the flexural rigidity of the considered plate, δ(x), δ(y) – the Dirac delta function along the X and Y axes, respectively, Vp(t) – voltage across the external resistive load R, while Γ – the electromechanical coupling term ($\Gamma = e_{31}(\frac{h_{plate}+h_{pe}}{2})$).

The considered plate, according to Fig. 1, has two simply supported edges oriented longitudinally to the Y axis whose boundary conditions are written in Eq. (2). As a result, considering these conditions, the eigen vectors of this structure are determined and expressed as:

$$w(x,y)=0; \quad \frac{\partial^2 w(x,y)}{\partial x^2}+\nu\frac{\partial^2 w(x,y)}{\partial y^2}=0; \quad \text{for } x=0,L \tag{2}$$

$$w(x,y)=\Theta_i\left[\begin{pmatrix}A_i ch\alpha_i y+B_i sh\alpha_i y+\\ C_i\alpha_i ch\alpha_i y+D_i\alpha_i sh\alpha_i y\end{pmatrix}\sin\alpha_i x\right] \tag{3}$$

where: $\alpha_i=\frac{i\pi}{L}$, i is i-th mode shape, Ai , Bi, Ci, Di - the coefficients of the vertical deflection individually determined for each mode shape, Θ_i - the modal amplitude constant.

Next, substituting the obtained Eq. (3) for Eq. (1) led to solving the eigenvalue problem of the smart plate for short circuit conditions (R→0). Then, the natural frequency ω_{mn} of the structure is simplified to the following form:

$$\omega_{mi}=\omega_i=\frac{\lambda_i\pi^2}{L^2}\sqrt{\frac{D}{\rho_p h_p}} \tag{4}$$

where: λ_i is the frequency parameter of an undamped plate.

From the energy harvesting system point of view, determining the differential equation of the coupled circuit dynamics is also an important step. For this purpose, the constitutive equation that governs the electrical circuit of the system has the following form:

$$C_p\frac{dV_p(t)}{dt}+\frac{V_p}{R}+\Gamma\left[\int_{y_{h1}}^{y_{h2}}\int_{x_{h1}}^{x_{h2}}\left(\frac{\partial^3 w(x,y,t)}{\partial x^2\,\partial t}+\frac{\partial^3 w(x,y,t)}{\partial y^2\,\partial t}\right)dxdy\right]=0 \tag{5}$$

where the capacitance of the piezo-patch is defined as:

$$C_p=\frac{\bar{\varepsilon}_{33}(x_{h2}-x_{h1})(y_{h2}-y_{h1})}{h_{peh}} \tag{5a}$$

By following the modal analysis procedure for Eq. (1) and Eq. (5), the electromechanically coupled ordinary differential equations of a 2D structure in modal coordinates can be written as:

$$\frac{d^2\eta_{mi}(t)}{dt^2}+2\xi_{mi}\omega_{mi}\frac{d\eta_{mi}(t)}{dt}+\omega^2{}_{mi}\eta_{mi}(t)-\tilde{\Gamma}_{mi}v(t)=f_{mi}(t)_1 \tag{6a}$$

$$C_p\frac{dV_p(t)}{dt}+\frac{V_p(t)}{R}+\sum_{m=1}^{\infty}\sum_{n=1}^{\infty}\tilde{\Gamma}_n\frac{d\eta_{mi}(t)}{dt}=0 \tag{6b}$$

where: ω_{mi} – the undamped short circuit of natural frequency for *mith* vibration mode, ξ_{mi} – the modal damping ratio, $f_{mi}(t)_1$ – the modal force derived from the piezo-actuator, $\tilde{\Gamma}_i$ – the modal electromechanical coupling term.

Then, both modal electromechanical coupling term and modal excitation force given by Eq. (6a) for the considered SFSF plate are expressed in the form:

$$\tilde{\Gamma}_i=\Gamma\left[\int_{y_{h1}}^{y_{h2}}\frac{\partial\phi_i(x,y)}{\partial x}\Big|_{x_{h1}}^{x_{h2}}dy+\int_{x_{h1}}^{x_{h2}}\frac{\partial\phi_i(x,y)}{\partial y}\Big|_{y_{h1}}^{y_{h2}}dx\right] \tag{7}$$

$$f_{mi}(t)_1=f_i(t)_1=\int_0^W\int_0^L f(t)\delta(x-x_{as1})\delta\left(y-\frac{y_{as2}-y_{as1}}{2}\right)\phi_i(x,y)dxdy+\int_0^W\int_0^L f(t)\delta(x-x_{as2})\delta\left(y-\frac{y_{as2}-y_{as1}}{2}\right)\phi_i(x,y)dxdy+2\int_0^W\int_0^L f(t)\delta\left(x-\frac{x_{as2}-x_{as1}}{2}\right)\delta\left(y-\frac{y_{as2}-y_{as1}}{2}\right)\phi_i(x,y)dxdy \tag{8}$$

Further analysis of the plate with integrated piezo-stripes in modal coordinates (Eq. (6a) and Eq. (6b)) leads to calculating the steady-state voltage response V(t) through the resistive load R expressed as:

$$V_p(\omega)=\frac{-j\omega\sum_{m=1}^{N}\sum_{i=1}^{N}\frac{C\tilde{\Gamma}_i}{\omega_{mi}{}^2+2j\xi_{mi}\omega_{mi}\omega-\omega^2}}{j\omega C_p+\frac{1}{R}+\sum_{m=1}^{N}\sum_{i=1}^{N}\frac{j\omega\tilde{\Gamma}_i{}^2}{\omega_i{}^2+2j\xi_{mi}\omega_{mi}\omega-\omega^2}} \tag{9}$$

where:

$$C=F_0\phi_i\left(x_{as1},\frac{y_{as2}-y_{as1}}{2}\right)+F_0\phi_i\left(x_{as2},\frac{y_{as2}-y_{as1}}{2}\right)-2F_0\phi_i\left(\frac{x_{as2}-x_{as1}}{2},\frac{y_{as}\ -y_{as1}}{2}\right)+F_0\phi_i\left(\frac{x_{as4}-x_{as3}}{2},y_{as3}\right)+F_0\phi_i\left(\frac{x_{as4}-x_{as3}}{2},y_{as4}\right)-2F_0\phi_i\left(\frac{x_{as4}-x_{as3}}{2},\frac{y_{as4}-y_{as3}}{2}\right)$$

3. FINITE ELEMENT MODEL

The numerical investigations of a rectangular aluminium plate with piezo-elements (harvester and actuator) attached to its surface were performed to determine a multi vibration mode equivalent circuit representation of the piezoelectric patch harvester connected to the resistive load. For this purpose, firstly, the eigenvalue problem of the structure is solved in the range of frequency up to 250 Hz containing the first five lowest mode shapes, because these modes are used to design a vibration control system of this structure in Koszewnik (2018) and Koszewnik and Gosiewski (2016). This led to the division of modes into odd and even ones and indicating which group of the lowest modes is the best one from the energy harvesting point of view.

In the next step, a proper harvester location on the plate is determined based on the analysis of mechanical strain fields and values of forces generated by the piezo-actuator for chosen mode shapes. In this study, the plate and piezo-stripes are modelled as a plane element (PLANE42), while epoxy glue as a spring-damper element (COMBIN14). As a result, the obtained numerical model is divided into 435 elements, each of them 25 mm long and 12.5 mm wide. By following the modal analysis procedure, the first five eigenvectors corresponding to eigenvalues are determined. The obtained mode shapes with natural frequencies are shown in Fig. 2.

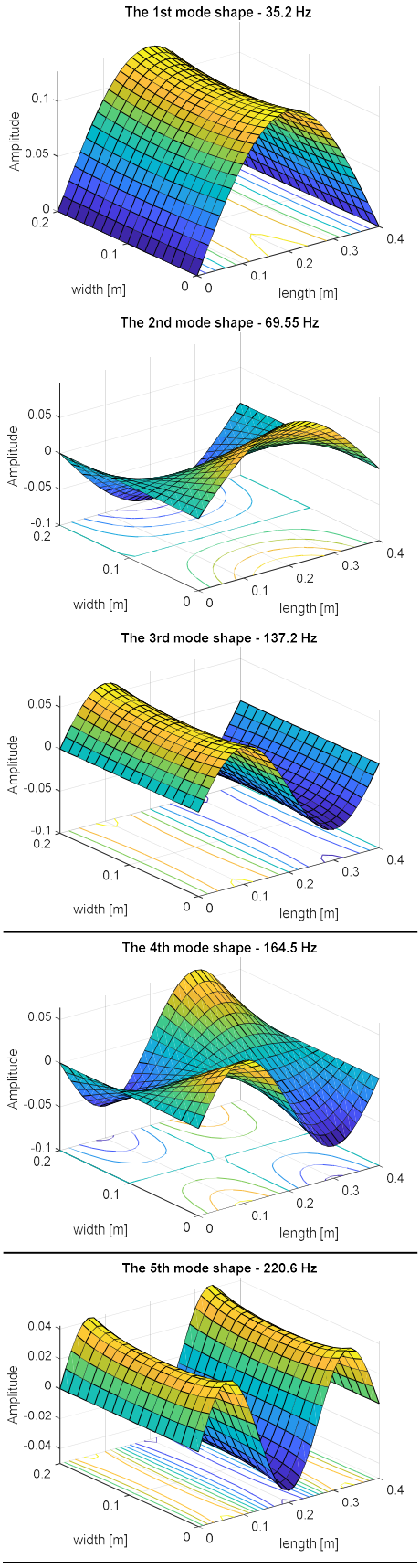

Fig. 2. The first five mode shapes of the transverse deformation for the SFSF plate in the frequency range 1–250 Hz (Koszewnik, 2018).

Fig. 2 shows the first five mode shapes of the transverse deformation of the smart plate with SFSF boundary conditions. As it can be seen in Fig. 2, the fundamental mode shape is in-phase on the overall surface with the maximum deflection placed at the half-length of this structure corresponding with the frequency of 35.2 Hz. In the case of two next modes, each of them has one node line in two perpendicular directions, respectively. The second mode (f2 = 69.5 Hz) has a node line longitudinally to Y axis at the centre of the plate, while the third mode (f3 = 137.2 Hz) at the centre of the X direction. Other modes (fourth and fifth) are totally different. The fourth mode has nodal lines located at the centre of the plate in both directions X and Y, respectively, while the fifth mode (f5 = 220.6 Hz) has also two nodal lines but they are located longitudinally to the Y axis.

Further analysis of modes' shapes in regard to the amount and direction of the nodes lines leads to assigning two kinds of modes, called 'odd modes' and 'even modes', respectively. As a result, the group of 'odd modes' is represented by only symmetrical modes located along the Y axis, while the 'even modes' – by modes symmetrically only along the X axis or screw-symmetrically versus X and Y axis.

The specified groups of mode shapes in the indicated frequency range 1–250 Hz allowed to determine a proper harvester location and orientation on the structure. For this purpose, the FE model was used again to calculate bending strain fields of the plate in two perpendicular directions X and Y, respectively.

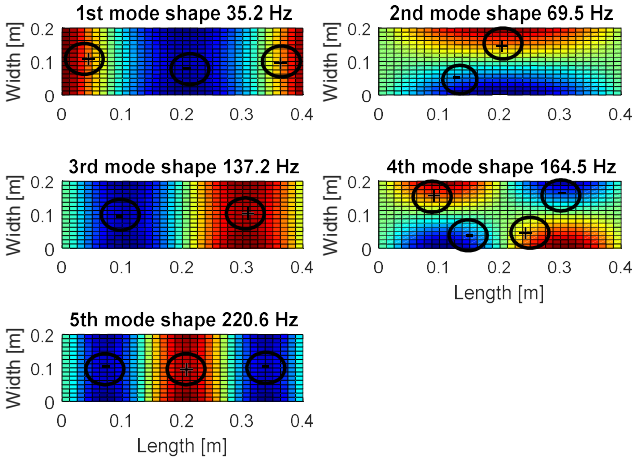

Fig. 3. The strain fields of the smart plate with an integrated piezo-stripes actuator and harvester for the first five mode shapes in *X* direction

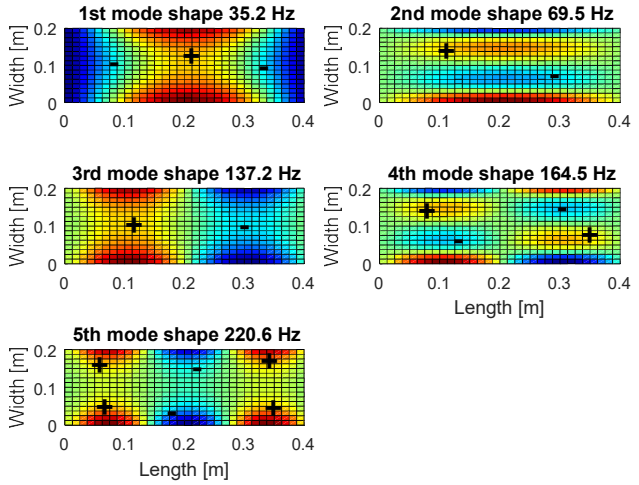

Fig. 4. The strain fields of considered plate with an actuator and harvester for the first five mode shapes in *Y* direction

DOI 10.2478/ama-2020-0002

The analysis of the obtained results shows that modal bending strain fields have strain nodal lines in both directions except for the fundamental mode of the plate first mode. From the energy harvesting point of view, it is a crucial problem because the output voltage is proportional to the strains. This implies that the output voltage generated by the harvester decreases dramatically when the piezoelectric stripe has a strain nodal line. Taking into account the electromechanical phenomena called voltage cancellation, it can be noticed that the longitudinal harvester orientations on the plate to the Y axis are less beneficial for the multi-vibration analysis. The harvester location in the proposed location (X = 0.10 m, Y = 0.05 m or X = 0.10 m, Y = 0.15 m) can be an exception, however, only for the second and the fourth modes. The strain fields in these areas are in-phase or out-of-phase. As a result, orienting the harvester only longitudinally to the X axis can be a better solution in this case. It is the consequence of the fact that this element can generate electrical outputs for almost all locations in the structure. Finally, the piezo harvester with a negligible effect on the strain distribution is placed at the left-lower quadrant of the plate in the distance of X = 20 mm from the simply-supported edge and Y = 50 mm from the free edge.

The indicated harvester locations and orientations on the host structure lead to calculating the modal value of the electromechanical coupling term Γ. For this purpose, based on Eq. (7), the modal value of this coefficient was calculated for each considered mode shapes. The obtained values of the electromechanical coupling term are collected and shown in Tab. 2.

Tab. 2. The value of modal elecromechanical coupling term determined for the five lowest natural frequencies

Mode shape	The electromechanical coupling term $\tilde{\Gamma}_i$
1st	-0.1231e-4
2nd	-0.0331e-4
3rd	-0.0593e-4
4th	-0.3096e-4
5th	-0.0604e-4

The modal force generated by the piezo-actuator is another parameter needed to calculate the DC voltage. For this purpose, the numerical model with a piezo-actuator located in the chosen places (see red rectangle in Fig. 5) on the plate are used again. In addition, the process of determining the piezo-actuator location is described in details in [22]. Each time it was assumed that the voltage applied to the piezo-actuators electrodes was 180 V, it allowed to generate a unit force in the indicated placement of the actuator and next, calculate the modal force fi(t) given by Eq. (8).

The analysis of the obtained results, presented in Fig. 5, show a significant increase of the modal forces values, especially for the odd modes. As a result, the process of determining a multi-mode representation of the Equivalent Circuit Model (ECM) is performed only for the first three odd mode shapes of the smart structure.

The obtained numerical results of the steady-state response of DC voltage are compared with a ECM model and shown in Fig. 9.

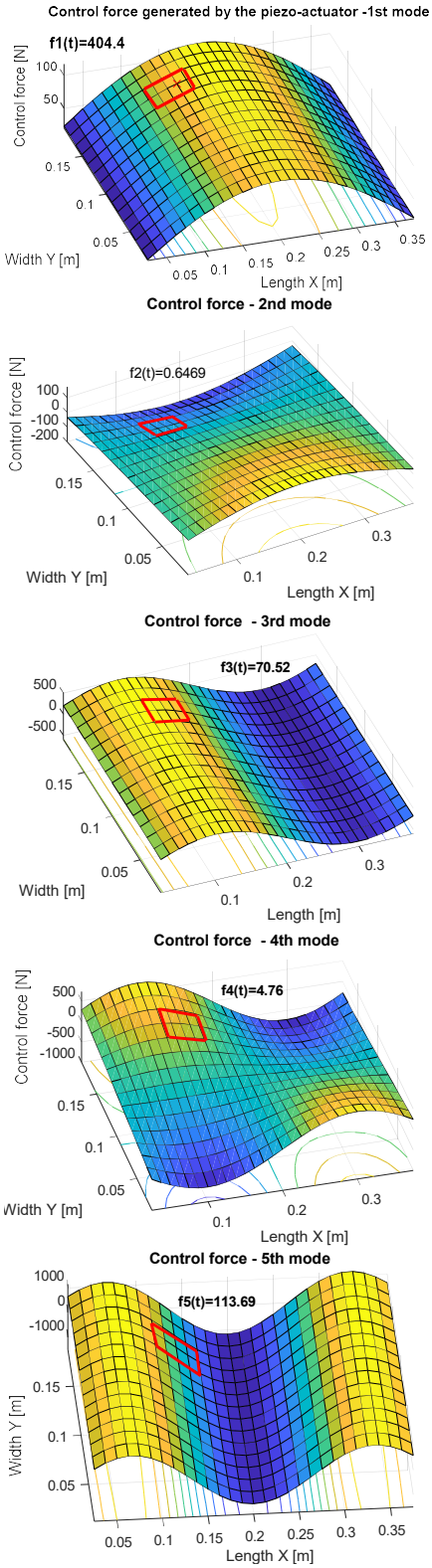

Fig. 5. The maximum amplitude of the modal force calculated for the piezo-actuator for the first five mode shapes

4. EQUIVALENT CIRCUIT MODELLING

The obtained distributed-parameters of the piezo-harvester integrated to the top surface of a 2D mechanical structure allowed to predict the power output with a good accuracy . It was achieved for the case when a linear component (e.g., resistor) is connected

to the system. Then, an equivalent circuit model (ECM) of the structure in the multi-mode is described by a finite number of lumped-parameters representing each vibration mode. In this case, the ECM model is composed of only three subsystems corresponding to the first odd mode shapes each of whom is described by the second order model. As a result, taking into account the electromechanical behaviour of the harvester, each vibration mode of the harvester is expressed by its capacitance (Cp), resistive load (R) and inductance (L), respectively. By applying Kirchhoff's Voltage Law to the multi-vibration mode circuit and by analogy with Eq. (6a), the parameters of the ECM model are identified and given by Eq. (10). Tab. 3 gives a summary of the analogy between the analytical distributed-parameter expression and the ECM, while Fig. 6 shows the comparison of both models, mechanical and ECM, in the frequency range of 1–250 Hz.

$$G_{ECM}(s) = \frac{s^3}{(s^2+4.42s+4.89e4)(s^2+9.24s+\ .55e5)(s^2+2.23s+\ .54e6)} \tag{10}$$

Tab. 3. Analogy between mechanical and electrical model of the piezo-stripe harvester

Parameters of mechanical model: $G_n(s)=\frac{W_n(s)}{F_n(s)}=\frac{k_n}{s^2+2\xi_n\omega_n s+\omega_n^2}$ **where:**	**Parameters of ECM** $G_{ECM,n}(s)=\frac{I_n(s)}{U_n(s)}=\frac{s}{Ls^2+R_n s+(1/C_n)}$ **where:**
Modal point force: $f_i(t)$	Modal voltage source: $V_i(t)$
1	Inductance: $L_i(t)$
$2\xi_{mi}\omega_{mi}$	Resistance: $R_i(t)$
$(1/\omega_{mi})^2$	Capacitance: $C_i(t)$
Γ_i	Transformer ratio: N_i
Modal time response: $\eta_{mi}(t)$	Electric charge: $Q_i(t)$
$\eta_{mi}(t)/dt$	Current $I_i(t)$

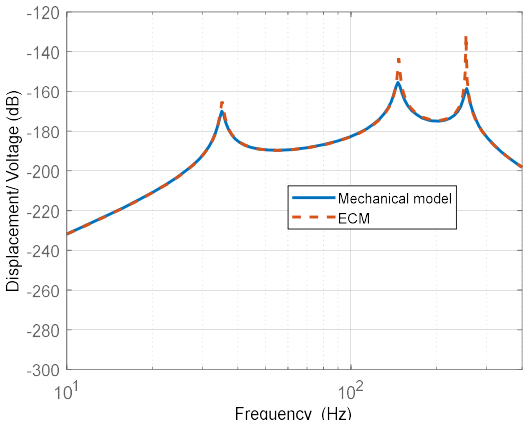

Fig. 6. The comparison of the amplitude plot of the mechanical model (experimental model) and the ECM model in the frequency domain containing three odd lowest frequencies' resonances

5. MODEL VALIDATION OF THE HARVESTER FOR THE STANDARD AC-DC PROBLEM

In this Section, an equivalent circuit model of an SFSF plate with perfectly bonded piezo-stripes QP20N and V21BL representing an actuator and a harvester is validated for the AC-DC standard problem from the electrical point of view (see Fig. 9b). In order to do this, the harvester on the lab stand, as it is shown in Fig. 7, is connected to a conditioning system EHE004 complex with a full-wave rectifier, a smoothing capacitor Cp = 100 μF and also the resistive load of R = 100 kΩ.

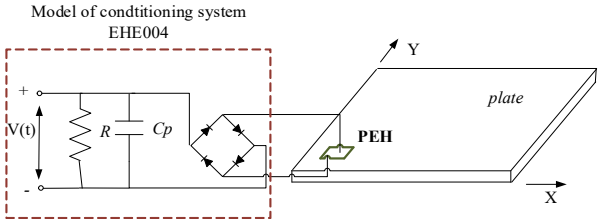

Fig. 7. The piezo-harvester V21BL connected to the EHE004 module

The experimental lab stand presented in Fig. 8a was also equipped with a bipolar voltage amplifier SVR-150bip/3 and a Digital Signal Analyzer (DSA). The amplifier is used to apply voltage (180 V) to the actuator, while the analyser – to measure and record the voltage output from the system.

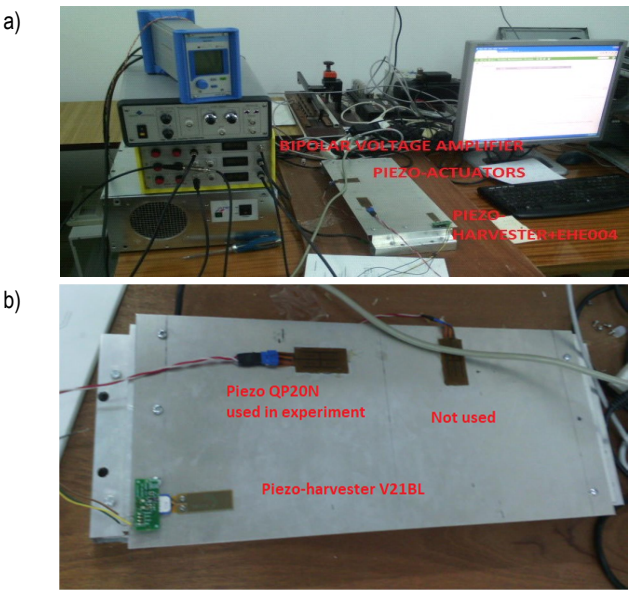

Fig. 8. a) The photo of the laboratory stand, b) the photo of a smart plate with piezo-elements (actuators QP10N and harvester V21BL) located on their top surface

The experimental set-up is carried out in a number of steps. In the first one, the structure is excited to vibration by using the piezo-actuator. For this purpose, a harmonic excitation signal in the form $u(t) = 2.5\sin(2\pi ft)$ is generated from DSA for a chosen natural frequency f_i of the structure (f_1 = 35.2 Hz, f_3 = 137.2 Hz, f_5 = 252.0 Hz), and next, it is applied to the actuator by the voltage amplifier. As a result, different values of the modal excitation force F_0 are obtained. From the measurement point of view, the vibration of the structure is measured by the harvester. The obtained AC voltage signals are rectified by the conditioning system EHE004 and then recorded by DSA. As a result, three steady state responses of DC voltages are obtained and shown in Fig. 9. In addition, the recorded signals are compared with the steady state response of DC voltages of ECM.

a)

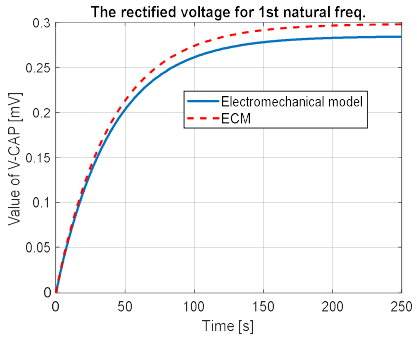

b)

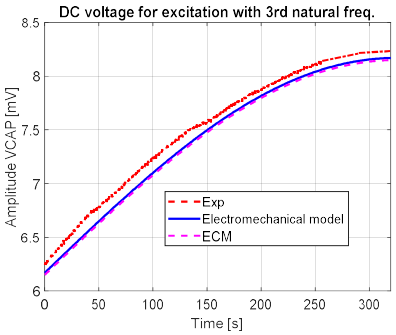

c)

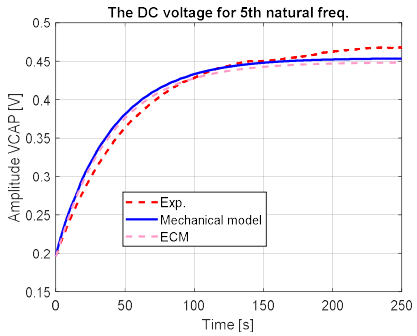

Fig. 9. Comparison of numerical (electromechanical model - blue line, Equivalent Circuit Model (ECM) - pink dash line) and experimental value (red dash line) of DC voltage obtained for the system excited to vibration with: a) 1st natural frequency, b) 3rd natural frequency, and c) 5th natural frequency

In the second step, the DC voltage is chosen as an indicator of the harvester effectiveness. Taking into account this indicator, it can be noticed that experimental results properly verified the numerical results. Especially, it is visible in Fig. 9b and Fig. 9c, where the values of voltage responses in the steady-state (8.5 mV for 3rd mode and 0.45 V for 5th mode) are close to the results obtained for ECM. In the case of the excitation system with the first natural frequency, the recorded voltage (less than 0.2 mV) was significantly lower than other result, and it was neglected. Further analysis of the obtained results showed that the filter capacitor Cp used in the system was not discharged enough. This leads to appearance of the offset value of DC voltages between tests. As a result, voltages for the electromechanical model and the equivalent circuit model were recalculated considering the ripple voltage and the capacitor discharge process. The corrected plots are shown in Fig. 9.

6. SUMMARY AND CONCLUSIONS

The thin SFSF plate with perfectly bonded piezo-patches is presented in the paper. Taking into account the chosen boundary conditions, the possibilities of the considered mechanical structure and the equivalent model to harvest energy are investigated. For this purpose, as the first step, the analysis of modes' shapes is carried out. The obtained results shown in Fig. 2 allowed to divide the considered modes into two groups according to the appearing node lines. In the next one, the bending strain fields of the smart plate in two perpendicular directions X and Y are considered. The numerical results shown in Fig. 3 and Fig. 4 indicated proper harvester locations and orientations on the structure for multi-vibration analysis. The calculated modal electromechanical coupling terms for the indicated harvester location allowed to assess the value of the steady state response of the DC voltage for an analytical model.

The obtained numerical results showed the effectiveness of the energy harvesting system only for the structure undergoing forced vibrations with only the first three odd natural frequencies. Taking into account this behaviour of the system, a multi-mode representation of the ECM model was determined only for the chosen vibration modes. By applying Kirchhoff's law and analogizing with Eq. (6a), parameters of the ECM model were determined.

Experimental tests carried out on the lab stand properly verified simulations results (see Fig. 9). The recorded steady state responses of DC voltage shows low effectiveness of the energy harvesting system beyond the case shown in Fig. 9c. This was caused by bigger dynamic strains' distributions appearing along the shorter edge of the plate. As a result, the generated voltage from the structure excited to vibration with the first or third natural frequency is not greater than 10 mV.

Summarizing, the performed investigations indicated that the harvester orientation on the 2D structure has its impact on the EH system properties. Further investigations of these systems connected with non-linear electrical components of the equivalent circuit model can lead to the increase of applying these systems in various types of civil infrastructure, especially in a range of structural health monitoring systems or powering other small devices with low power demand. Thus, taking the proposed approach into account, future research will be focused on an EH system located on the front wall of a dishwasher without a bitumen damper. As a result, this will lead to obtaining structural health monitoring systems of such mechanical structures.

REFERENCES

1. **Aboulfotoh N., Wallscheck J., Twiefel J., Bergman L.**, (2017), Toward understanding the self-adaptive dynamics of a harmonically forced beam with a sliding mass, *Archive of Applied Mechanics*, 87(4), 699–720.
2. **Ambrożkiewicz B., Litak G., Wolszczak P.**, (2020), Modelling of Electromagnetic Energy Harvester with Rotational Pendulum using Mechanical Vibrations to Scavenge Electrical Energy, *Applied Sciences*, 10(2), 671.
3. **Anton Novel SR.**, (2009), Piezoelectric Energy Harvesting Devices for Unmanned Aerial Vehicles, *Smart Material Structures*, 1–10.
4. **Anton SR.,** (2011), Multifunctional Piezoelectric Energy Harvesting Concepts, Doctoral Thesis, Virginia Polytechnic Institute and State University.
5. **Borowiec M.,** (2015), Energy harvesting of cantilever beam system with linear and nonlinear piezoelectric model, *The European Physical Journal – Special Topics*, 224, 2771–2786.
6. **Cahill P., Nuallian N., Jackson N., Mathewson A., Karoumi R., Pakrashi V.,** (2014), Energy Harvesting from Train-Induced Response in Bridges, *ASCE Journal of Bridge Engineering*, 04014034.

7. **Cahill P., Nuallian N., Jackson N., Mathewson A., Karoumi R., Pakrashi V.**, (2018), Vibration energy harvesting based monitoring of an operational bridge undergoing forced vibration and train passage, *Mechanical System and Signal Processing*, 106, 265–283
8. **Chiu Y., Tseng V.,** (2008), A capacitive vibration-to-electricity energy converter with integrated mechanical switches, *Journal of Micromechanics and Microengineering*, 18(10), 104004.
9. **Cook-Chennault K., Thambi N., Sastry S.,** (2007), Powering MEMS portable devices – a review of non-regenerative and regenerative power supply systems with special emphasis on piezoelectric energy harvesting systems, *Smart Material and Structures*, 16(3), 043001.
10. **De Marqui C.,** (2011), Modelling and analysis of piezoelectric energy harvesting from aeroelastic vibrations using the doublet-lattice method, *Trans. ASME Journal of Vibration Acoustic*, 133, 011003.
11. **Gosiewski Z.,** (2008), Analysis of Coupling Mechanism in lateral/torsional Rotor Vibrations, *Journal of Theoretical and Applied Mechanics*, 46(4), 829–844.
12. **Hanre RL**., (2012), Concurrent attenuation of and energy harvesting from, surface vibrations: experimental verification, and model validation*, Smart Material Structures*, 21, 035016.
13. **Hanre RL.,** (2013), Development and testing of a dynamic absorber with corrugated piezoelectric spring for vibration control and energy harvesting applications, *Mechanical System and Signal Processing*, 36(2), 604–617.
14. **Hu Y. , Zhang Y.** (2011), Self-powered system with wireless data transmission, *Nano Letters*, 11(6), 2572–2577.
15. **Koszewnik A**. (2016), The optimal vibration Control of the Plate Structure by using piezo-actuators, Proceedings of the 17th IEEE International Carpathian Control Conference (ICCC), Tatrzanska Lomnica, Slovakia, 358–363
16. **Koszewnik A.** (2018), The Design of Vibration Control System for Aluminum Plate with Piezo-stripes based on residues analysis of model, *European Physical Journal Plus*, 133:405.
17. **Koszewnik A.** (2019), Analytical Modelling and Experimental Validation of an Energy Harvesting System for the Smart Plate with an Integrated Piezo-Harvester, *Sensors*, 19, 812.
18. **Koszewnik A., Gosiewski Z**. (2016) Quasi-optimal locations of piezo-elements on a rectangular plate, *European Physical Journal Plus*, 2016, 131:232.
19. **Koszewnik A., Wernio K.** (2016), Modelling and Testing of the piezoelectric beam as energy harvesting beam, *Acta Mechanica et Automatica*, 10(4), 291–295.
20. **Lee Ch., Lim Y.M., Yang B.** (2009), Theoretical comparison of the energy harvesting capability among various electrostatic mechanisms from structure aspect, *Sensor Actuator A*, 156(1), 208–216.
21. **Litak G., Borowiec M., Fischer M., Przystupa W**., (2009), Chaotic response of a quarter car model forced by a road profile with a stochastic component, *Chaos, Solutions and Fractals*, 9, 2448–2456.
22. **Naifar S., Bradai S., Viehweger C., Kanoun O**., (2015), Response analysis of a nonlinear magnetoelectric energy harvester under harmonic excitation, *The European Physical Journal – Special Topics*, 224, 2879–2908.
23. **Okosun F., Cahill P.,Hazra B., Pakrashi V.**, (2019), Vibration-based leak detection and monitoring of water pipes using output–only Piezoelectric Sensors, *European Physical Journal – Special Topics*, 228, 1659–1675.
24. **Roundy W., Wright P., Rabaey J.**, (2003), A study of low level vibrations as a power source for wireless sensor nodes*, Computer Communications*, 26, 1131–1144.
25. **Wang L., Yuan F.G.,** (2008), Vibration energy harvesting by magnetostrictive material, *Smart Materials and Structures*, 17, 045009.

This work is supported with University Work number WZ/WM-IIM/1/2019 of Faculty of Mechanical Engineering, Bialystok University of Technology.